IV International Conference on Particle-based Methods – Fundamentals and Applications
PARTICLES 2015
E. Oñate, M. Bischoff, D.R.J. Owen, P. Wriggers& T. Zohdi(Eds)

A MOLECULAR DYNAMICS STUDY ON THE EFFECTS OF WALL-FLUID INTERACTION STRENGTH AND FLUID DENSITY ON THERMAL RESISTANCE OF GRAPHENE/ARGON INTERFACE

AHMAD AMANI[1], S.M.H. KARIMIAN[1]AND MAHBOD SEYEDNIA[2]

[1] Department of Aerospace Engineering, Amirkabir University of Technology
424 Hafez Ave., Tehran, Iran, 15875-4413
ahmad.amani@aut.ac.ir, hkarim@aut.ac.ir

[2] Faculty of New Sciences and Technologies, University of Tehran
North Kargar Ave., Tehran, Iran, 14395-1561
m.seyednia@ut.ac.ir

Key words: Molecular Dynamics, Interface Thermal Resistance, Kapitza Length, Confined Argon Flow.

Abstract. Molecular dynamics simulations of Argon flow confined between two parallel graphene sheets are carried out to investigate the effects of some parameters on heat transfer and thermal properties. These parameters include wall-fluid interaction strength and fluid density where for constant wall temperature simulations, we show that these two parameters have influence on near-wall fluid density. As a result, the heat transfer at wall-fluid interfaces and thus through Argon molecules across the domain will change. To analyze the results, the density and temperature profiles and two other parameters including temperature gradient of the bulk of Argon molecules and the Kapitza length are considered. The Kapitza length represents the thermal resistance at liquid-solid interface. According to the results, the increase of wall-fluid interaction strength leads to greater number of Argon molecules near the walls and consequently, the Kapitza length decreases and an enhancement is observed in temperature gradient and the slope of temperature profile. Furthermore, higher values of fluid density cause that the thermal resistance at wall-fluid interactions increases. Therefore, greater temperature jumps are observed in temperature profiles.

1 INTRODUCTION

Molecular dynamics (MD) simulation of fluid flows in micro/nano sizes has been widely developed to extract detailed information on fluid behavior, especially in medicine, physiology, and nano scale devices [1-4]. Micro-electro-mechanical-systems (MEMS) and Nano-electro-mechanical-systems (NEMS) are such devices which have commercial applications [5] so it is necessary to have a comprehensive perception of thermal transport in these systems. As a result, molecular dynamics approach is implemented to model the heat transfer in nanostructures. In the researches of this field, temperature profile, calculation of heat flux, interface thermal resistance (ITR), thermal conductivity, and thermal efficiency of

various structures are subjected to study [6-13]. Most analyses of these results treat conduction as a diffusion process which can be described by Fourier's law and confirm that the interface thermal resistance strongly affects the heat transfer.

Two theoretical models lead the interpretation of this phenomenon. Acoustic mismatch model (AMM) was proposed by Little [14] which predicted the thermal resistance by treating the phonons as plane waves with assumption that no scattering occurs at the interface. Swartz and Pohl [15] proposed diffusive mismatch model (DMM) which assumes that diffuse scattering destroys acoustic effects at interface. In a solid/liquid interface, two parameters of temperature and near-surface structure of liquid affect the ITR.

Nano scale Poiseuille flows have been subjected to investigate the effects of different parameters on Interface thermal resistance. Shi et al. studied thermal resistance at argon-graphite and argon-silver interfaces [16]. Barisik and Beskok investigated the interface thermal resistances and represented a range for interface thermal resistance of argon-silver interface [17] and also investigated the effect of different silicon-water interaction strength values on the Kapitza length [18]. According to Murad and Puri reports, increase of the fluid pressure or fluid molecule layers will decrease the Kapitza length [19]. In spite of a wide range of knowledge in the discussed field, the affecting parameters on interface thermal resistance of argon flow confined between graphene [20] sheets is not clear.

In this paper, two different parameters including wall-fluid interaction strength and fluid density which have influence on the heat transfer and the thermal properties of an Argon flow confined between two parallel graphene sheets are investigated. We are interested to find out how these parameters affect the thermal properties. The effects of them are represented by plotting the density and temperature profiles. Heat flux, temperature gradient and the Kapitza length will be studied to compare the results and make a conclusion. In the following part, the simulation and the parameters considered in this paper are described and in chapter 3, the results are presented.

2 MOLECULAR DYNAMICS SIMULATION DETAILS

A liquid Argon flow confined between two parallel graphene sheets is simulated. Using LAMMPS solver [21], the mono atomic noble gas molecules of Argon are located in the domain in a way that the particle density [22] is 0.85. However it will be changed for more analysis in 3.2. The particle density is calculated as:

$$\rho^* = \frac{N}{L_1^{'}.L_2^{'}.L_3^{'}} \tag{1}$$

where N is the number of molecules and $L^{'}$ is the dimensionless length. It is noteworthy that the particle density can be calculated for the bins and the whole domain.

Total dimensions of the domain are 3.40, 3.46 and 4.34 nm in X, Y and Z directions respectively. Periodic boundary conditions are applied on X and Y directions and Z direction is limited by the graphene sheets. As wall structure, the graphene sheets consist of 448 carbon atoms arranged in Hexagonal lattice with separation of 0.142 nm. In order to avoid the escape of the fluid molecules, the wall molecules are attached to their initial positions by a linear spring with the stiffness of $500\varepsilon / \sigma^2$ .Using VMD [23], the initial placement of the molecules is depicted in figure 1.

The motions of the molecules are determined by Newton's second law using Verlet's integrating schemes [24-25] with a time step of 1 femtosecond. The intermolecular interactions of Carbon-Carbon molecules are calculated using Adaptive Intermolecular Reactive Empirical Bond Order (AIREBO) potential. AIREBO potential includes three different potentials; REBO, Lennard-Jones and TORSION. The REBO term is a hydrocarbon potential describing the short-range interactions of carbon-carbon molecules. The longer-ranged interactions of carbon-carbon molecules are calculated by The Lennard-Jones term and the TORSION is a 4-body potential which describes the dihedral angle preferences in graphene structure. Implementing Lennard-Jones (L-J) 6-12 potential function, the intermolecular forces between the fluid-fluid molecules are calculated as below [26]:

$$U_{ij} = 4\varepsilon\left(\left(\frac{\sigma}{r_{ij}}\right)^{12} - \left(\frac{\sigma}{r_{ij}}\right)^{6}\right) \tag{2}$$

where U_{ij} is L-J potential, σ is the distance characteristic length, ε is the energy scale and r_{ij} is the distance between two interacting molecules i and j. The derivation of the above equation respect to r_{ij} is applied to calculate the intermolecular forces. The energy scale, ε, for Argon is 0.0103403 ev. The wall-fluid interactions are calculated by Lennard-Jones as well as fluid-fluids. Nevertheless, it is noteworthy that the energy scale and the distance characteristic length must be changed to appropriate values. Implementing mixing rule, the distance characteristic length and the energy scale for wall-fluid interactions are 3.268 Å and 0.00557256 ev respectively. This value of ε will be referred as ε_b in the next sections.

Initial temperature of 130 K is set for Argon molecules. Applying Maxwell-Boltzmann distribution function on the Argon molecules, the initial thermal velocities are randomized. To reach thermal equilibrium, we let the system iterate for 10^6 times (1 ns) while Canonical (NVT) ensemble with Nose-Hoover thermostat is applied on the whole molecules keeping the temperature of the system at 130 K. Afterward, in order to induce a heat flux through the domain, top and bottom wall temperatures are assigned 150 and 110 K, respectively using Nose-Hoover thermostat while NVE ensemble is applied to the water molecules for 2×10^6 iterations (2 ns) to ensure that the system attains equilibrium with the new heat flux conditions. Then, 3×10^6 iterations (3 ns) are considered for averaging to obtain macroscopic properties. The sampling is performed in 29 and 59 slab bins parallel to the graphene sheets to attain temperature and density profiles respectively. The Lennard-Jones potential predicts repulsive forces as the distance between two molecules decreases less than the potential minimum length. Hence, the bins adjacent to the graphene sheets would be unoccupied by the Argon molecules or the number of Argon molecules is not sufficient for sampling. Therefore the adjacent bins are left out in local temperature averaging whereas there would be no omission in the density bins. In other bins with low number of molecules, the results would not be reliable. So for such a bin, a linear interpolation of temperature between the corresponding adjacent bins is implemented to make the temperature profiles continuous. The interpolated temperatures for these bins are calculated and they are marked with a box around in temperature profiles.

Different temperatures for graphene sheets will lead to a thermal gradient in Z direction. As a result, this gradient generates heat flux between the parallel sheets. The rate of heat transfer can be calculated as below:

$$\vec{j} = \frac{1}{V}\left(\sum_i e_i v_i + \sum_{i<j} \left(f_{ij} . v_j \right) r_{ij} \right) \tag{3}$$

where V is the volume of the domain and e_i and v_i denote the total energy per atom and the velocity of particle i while f_{ij} and r_{ij} represent the force caused by molecule j which acts on molecule i and the distance between two interacting molecules respectively.

In order to calculate the Kapitza length at the liquid-solid interfaces, an extrapolation is performed on temperature profile from liquid into the solid where the wall temperature is reached. The Kapitza length can be calculated using:

$$\Delta T = L_K \left. \frac{\partial T}{\partial n} \right|_{liquid} \tag{4}$$

where $\frac{\partial T}{\partial n}$ is the temperature gradient on the liquid side and $\Delta T = T_{liquid} - T_{wall}$. In order to analyze thermal properties, Kapitza lengths, the heat flux generated between the walls and the temperature gradient of argon molecules across the domain are studied. In each case, the particles are distributed uniformly over the simulation domain with the corresponding particle density. Two parameters of ε_{C-O}^{LJ} and r_{cut} are the major sources of uncertainties in the system analyzed in this paper. More information about these parameters could be found in Ref [27].

3 RESULTS AND DISCUSSION

In this paper, two different parameters are investigated to study their influences on thermal properties of the mentioned Argon flow. These parameters include wall-fluid interaction strength and fluid density. Temperature and density profiles, temperature gradient plots and Kapitza lengths are utilized to analyze the thermal properties in each case.

3.1 Effect of wall-fluid interaction strength

To investigate the effect of wall-fluid interaction strength, five different interaction strength values including 1, 2, 4, 6, 8 and $10 \times \varepsilon_b$ are considered. The density profiles of each case are depicted in figure 2. Using equation (1), the dimensionless densities are calculated in all the bins for each case. Although it cannot be seen in the figure 2, the density profiles across the channel are not totally symmetric. The particle density of the bins near the upper wall (with higher temperature) is slightly greater than that of the bins adjacent to the lower wall (with lower temperature). It represents the influence of wall temperature on distribution of Argon molecules. This is due to the fact that the molecular motions in the upper layers are greater than those of in the lower layers. Higher molecular motions cause a partial reduction in number of Argon molecules occupying a bin. So the upper bins contain fewer Argon molecules rather than the corresponding lower bins.

According to the Carbon-Argon interactions and their interaction strength, the Argon molecules are repelled or attracted by the Carbons. As a result, different density profiles are obtained for different values of wall-fluid interaction strength. The fluctuations in density profiles are caused by density layering of the Argon molecules near the walls. Getting away from the walls, the fluctuations are decaying and the density is approaching to the initial value of 0.85. Increase of wall-fluid interaction causes more attraction of Argon molecules in near-wall bins. Different density profiles for different interaction strengths affect the thermal properties such as temperature profile, Kapitza length and heat flux of the bulk of Argon molecules.

The temperature profiles obtained using the mentioned slab bins are plotted in figure 3. It is noticeable that different values of wall-fluid interaction strength result in different temperature plots and in all cases, temperature jump can be seen at liquid-solid interfaces. These jumps can be associated with phonon mismatch at the interfaces. The increase of interaction strength leads to more concentration of Argon molecules near the walls and consequently better coupling between the Argon and Carbon molecules. As a result, the temperature of the near-wall Argon molecules would be closer to the corresponding wall temperature and thus the temperature gradient of Argon molecules across the channel increases. The increase in the slope of the temperature profile is the evidence of this phenomenon. The curvature of the profiles can be attributed to thermal conductivity as a function of temperature. It was mentioned in section 2 but it is worth pointing out again that the temperatures marked in a box are the bins with insufficient number of molecules where their temperatures are obtained by linear interpolation.

For more accurate analysis of the temperature profiles, we consider the other parameters mentioned above. The results are extracted from the simulations to make a better study of thermal properties. The temperature gradient of Argon molecules across the channel is plotted in figure 4 for different values of interaction strength. The temperature gradient is obtained by calculation of the slope of the temperature profile. The method of least squares is implemented for curve fitting and the calculation of the slope. The square residuals for all cases are less than 2.5%. According to figure 4, the increase of ε_{Ar-C} enhances the temperature gradient of the bulk of Argon molecules. This is because of the enhancement in the slope of temperature profile which was explained before. Another parameter studied for thermal properties investigation is the heat flux transported between Argon molecules. The amounts of heat flux between the walls are also depicted in figure 4. It is noticeable that the heat flux increases by higher interaction strength as well as the temperature gradient.

As mentioned in section 1, Kapitza length is a parameter representing thermal resistance. For all cases of different interaction strengths, this length has been calculated for two liquid-solid interfaces and the results are plotted in figure 5. Clearly from this figure, there is an inverse relationship between ε_{Ar-C} and Kapitza length. The increase of ε_{Ar-C} reduces the Kapitza length and therefore the thermal resistance at the interfaces as well. Higher amount of ε_{Ar-C} induces more interactions between the Argon and Carbon molecules at the interfaces. Hence, better coupling and heat transfer between these molecules occur. Moreover, it is obvious that the Kapitza length for the upper wall (with higher temperature) is less than that of the lower wall. This is due to the fact that higher temperature dominates the interface thermal conductivity and consequently the Kapitza length.

3.2 Effect of density

The influence of density on thermal properties is investigated in this part. Different values of particle density including 0.65, 0.75, 0.85 and 0.95 have been considered to study if particle density affects thermal properties.

A dimensionless particle density is utilized to plot the number of atoms in each bin across the channel. To investigate the distribution of Argon molecules due to different densities and compare density profiles, the number of Argon molecules in each bin for all cases has been calculated. By dividing the number of particles in each bin by the total number of Argon molecules, we can compare the density profiles. The resultant value is multiplied by 100 and hence the result indicates the percentage of Argon molecules that each bin contains in each case of particle density. Now it would be possible to study the effect of density in the bins across the channel. Figure 6 illustrates the percentage of Argon molecules across the channel for different particle densities.

As it was mentioned earlier, the distribution and the concentration of fluid molecules near the walls affect the temperature jump at the interface of wall and fluid. From figure 6, it is self-evident that increasing density leads to decrease in the percentage of Argon molecules near walls. In other words, higher fluid density increases the concentration of molecules in the middle of the domain rather than near the walls. Therefore lower slope of temperature profile across the domain is expected for higher densities which represents decreasing in temperature gradient of Argon molecules between the walls and the Kapitza length as well. The temperature profiles for different values of particle density are plotted in figure 7. The results for the temperature profiles confirm the fact that increasing fluid density decreases the temperature slope and temperature gradient.

It was mentioned in previous part that the temperature gradient of Argon molecules corresponding to each particle density is obtained by the slope of the temperature profiles. The temperature gradients for different particle densities are depicted in figure 8. As evident from this figure, higher density accompanies by lower temperature gradient. Furthermore, increasing the density enhances the Kapitza length at the interface of the fluid and the walls. Figure 9 shows the variations Kapitza length with particle density. The enhancement in Kapitza length can interpret as increase in interface thermal resistance between the fluid and the walls. The reason of the difference between the Kapitza lengths at two interfaces was mentioned in 3.1.

The amounts of heat flux generated across the channel through Argon molecules for different particle density are shown in figure 10. According to figure 10, the heat flux through Argon molecules has a direct relationship with fluid density. This can be interpreted by using the one-dimensional model of heat conduction, Fourier's law. Below is the one-dimensional form of the Fourier's law:

$$Q_z = -kA_c \frac{dT}{dZ} \tag{5}$$

Where Q_z is the heat flux induced in the Z direction, k is thermal conductivity, A_c is cross-sectional area of the heat flux and $\frac{dT}{dz}$ is applied temperature gradient. Due to this equation,

the two parameters, k and $\frac{dT}{dz}$, have influence on heat flux. According to the temperature profiles, the temperature gradients and the Kapitza lengths presented above, as fluid density increases, the interface thermal resistance increases as well. Hence, the temperature gradient of the bulk of Argon molecules decreases. Nonetheless, the induced heat flux through Argon molecules increases which is attributed to the enhancement of thermal conductivity of the bulk of Argon molecules.

4 CONCLUSION

In this paper, we showed that heat transfer and thermal properties at wall-fluid interfaces are as function of near-wall fluid density and wall temperatures. To prove this claim, two parameters including wall-fluid interaction strength and fluid density were considered to analyze the thermal properties of an Argon flow through two parallel graphene sheets. We showed that the these two parameters have influence on fluid density at near wall regions and consequently the thermal properties

The results clearly showed that increase of wall-fluid interaction strength raises the number of fluid molecules near the walls. Higher interaction strength creates better coupling between the Argon and Carbon molecules and thus the slope of temperature profile increases. As a result, the Kapitza length decreases and the temperature gradient of Argon molecules across the system rises.

The studies on the effect of fluid density on thermal properties also indicated that increasing fluid density will change the distribution of fluid molecules near the walls in a way that the interface thermal resistance increases. As a result, the interface thermal conductivity decreases and the temperature jump between the wall and the fluid is enhanced. However higher fluid densities cause an increase in fluid-fluid interactions and thermal conductivity in the bulk of Argon molecules as a consequence.

REFERENCES

[1] Cruz-Chu, E.R., Malafeev, A., Pajarskas, T., Pivkin, I.V. and Koumoutsakos, P., Structure and Response to Flow of the Glycocalyx Layer, *Biophysical Journal*, (2014) **106**:232-243

[2] Bresme, F. and Römer, F., Heat transport in liquid water at extreme pressures: A non equilibrium molecular dynamics study, *Journal of Molecular Liquids*, (2013) **185**:1-7

[3] Castillo-Tejas, J., Castrejón-González, O., Alvarado, J.F.J. and Manero, O., Prediction of excess pressure drop in contraction–expansion flow by molecular dynamics: Axisymmetric and planar configurations, *Journal of Non-Newtonian Fluid Mechanics*, (2014) **210**:1-11

[4] Adelman, J.L., Sheng, Y., Choe, S., Abramson, J., Wright, E.M., Rosenberg, J.M. and Grabe, M., Structural Determinants of Water Permeation through the Sodium-Galactose Transporter vSGLT, *Biophysical Journal*, (2014) **106**:1280-1289

[5] Karniadakis, G.E, Beskok, A., and Aluru, N., *Micro flows and Nano flows*, Springer, (2002) New York, 1-9.

[6] Zhang, G. and Li, B., Thermal Conductivity of Nanotubes Revisited: Effects of Chirality, Isotope Impurity, Tube Length, and Temperature, *J. Chem. Phys.* (2005) **123**:114714.

[7] Yao, Z., Wang, J.S., Li, B. and Liu, G.R., Interface thermal resistance and thermal

conductivity in composites, *Phys. Rev. B* (2005) **71**:085417.
[8] Wu, G. and Li, B., Thermal rectification in carbon nanotube intramolecular junctions: Molecular dynamics calculations, *Phys. Rev. B* (2007) **76**:085424.
[9] Donadio, D. and Galli, G., Thermal Conductivity of Isolated and Interacting Carbon Nanotubes: Comparing Results from Molecular Dynamics and the Boltzmann Transport Equation, *Phys. Rev. Lett.* (2007) **99**:255502.
[10] Jiang, J.W., Wang, J.S. and Li, B., Topology-induced thermal rectification in carbon nanodevice, *Europhys. Lett.* (2010) **89**:46005.
[11] Hu, J., Ruan, X. and Chen, Y.P., Thermal Conductivity and Thermal Rectification in Graphene Nanoribbons: A Molecular Dynamics Study, *Nano Lett.* (2009) **9**:2730.
[12] Zhang, G.P. and Qin, Z.J., Crossover of the conductivity of zigzag graphene nanoribbon connected by normal metal contacts, *Phys. Lett. A* (2010) **374**:4140.
[13] Murad, S. and Puri, I.K., Interface thermal resistance and thermal conductivity in composites – an abrupt junction thermal diode model, *Phys. Lett. A* (2010) **374**:4242.
[14] Little, W.A., The transport of heat between dissimilar solid at low temperature, *Can. J. Phys* (1959) **37**:334±349.
[15] Swartz, E.T. and Pohl, R.O., Thermal boundary resistance, *Reviews of Modern Physics* (1989) **61**:605±668.
[16] Shi, Z., Barisik, M. and Beskok, A., Molecular dynamics modeling of thermal resistance at argon-graphite and argon-silver interfaces, *International Journal of Thermal Sciences*, (2012) **59**:29-37
[17] Barisik, M. and Beskok, A., Boundary treatment effects on molecular dynamics simulations of interface thermal resistance, *J. Comput. Phys*., (2012) **231**:7881-7892
[18] Barisik, M. and Beskok, A., Temperature dependence of thermal resistance at the water/silicon, (2014) **77**:47-54
[19] Murad, S. and Puri, I.K., Thermal transport across nanoscale solid-fluid interfaces, *Applied Physics Letters*, (2008) **92**:133105
[20] Novoselov, K.S., Geim, A.K., Morozov, S.V., Jiang, D., Zhang, Y., Dubonos, S.V., et al., Electric field effect in atomically thin carbon films, *Science*, (2004) **306**:666-669
[21] Plimpton, S., Fast Parallel Algorithms for Short-Range Molecular Dynamics, *J Comp Phys*, (1995) **117**:1-19
[22] Karimian, S.M.H. and Amani, A., A proposal for the implementation of symmetry boundary condition In molecular dynamics simulation, *Proceedings of the third European Conference on Microfluidics, Heidelberg, Germany, December* (2012), 246.
[23] Humphrey, W., Dalke, A. and Schulten, K., VMD - Visual Molecular Dynamics, *J. Molec. Graphics,* (1996) **14**:33-38
[24] Allen, M.P. and Tildesley, D.J.,*Computer Simulation of Liquids*,Clarendon Press, (1989)
[25] Swope, W.C., Andersen, H.C., Berens, P.H. and Wilson, K.R., A computer simulation method for the calculation of equilibrium constants for the formation of physical clusters of molecules, *The Journal of Chemical Physics*, (1982) **76**:637-649
[26] Che, J.W., Cagin, T. and Goddard, W.A., Thermal conductivity of carbon nanotubes, *Nanotechnology*, (2000) **11**:65-69
[27] Angelikopoulos, P., Papadimitriou, C. and Koumoutsakos, P., Data Driven, Predictive Molecular Dynamics for Nanoscale Flow Simulations under Uncertainty, *The Journal of Physical Chemistry B*, (2013), **117**:14808−14816.

FIGURES

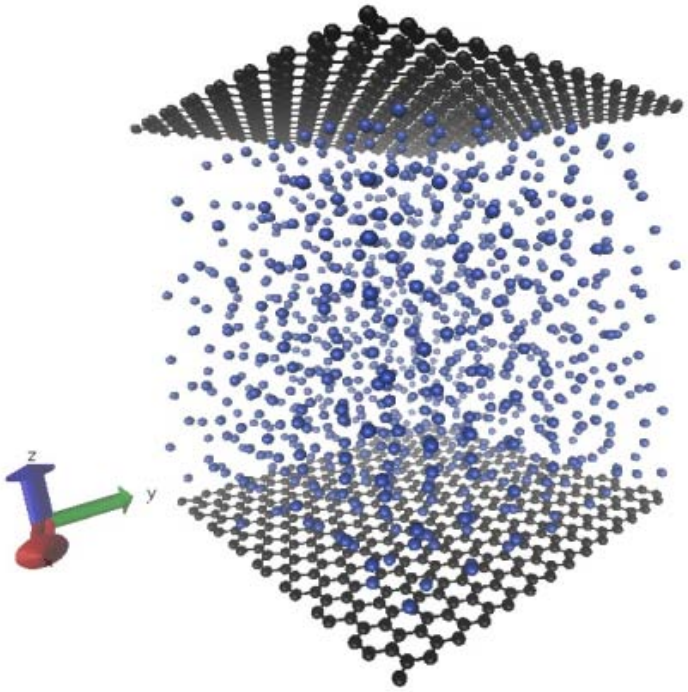

Figure 1: Schematic of initial molecules positions

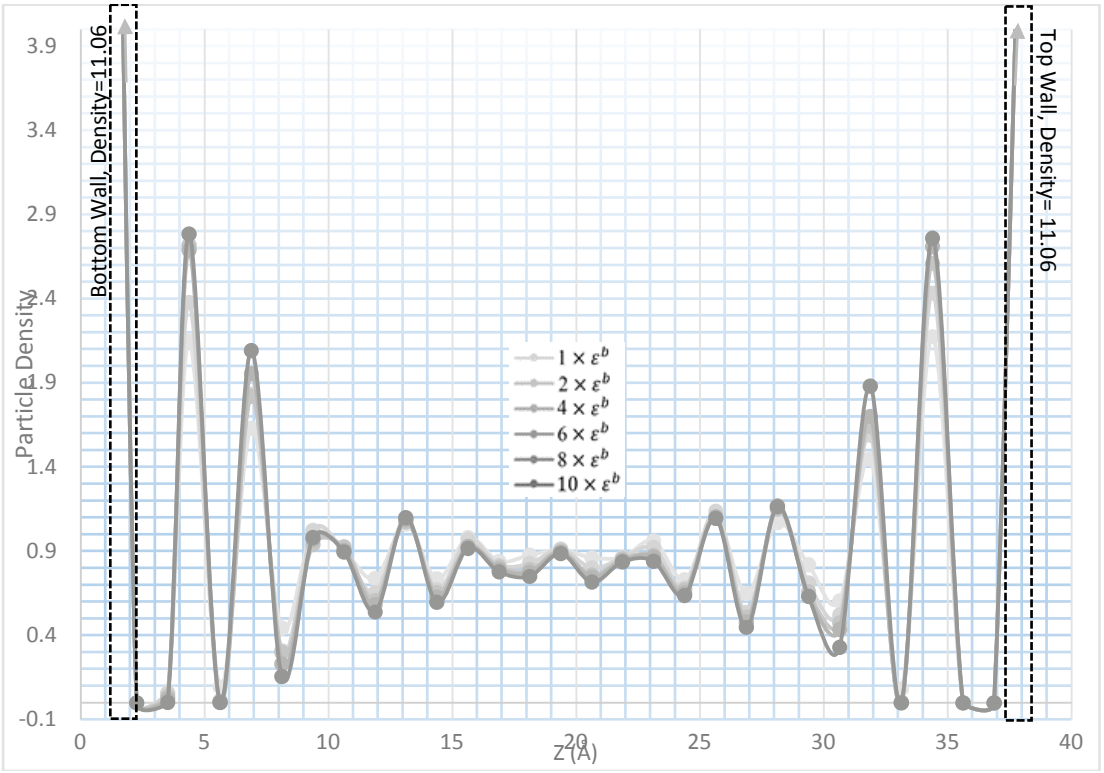

Figure 2: Particle density profiles of different values of wall-fluid interaction strength

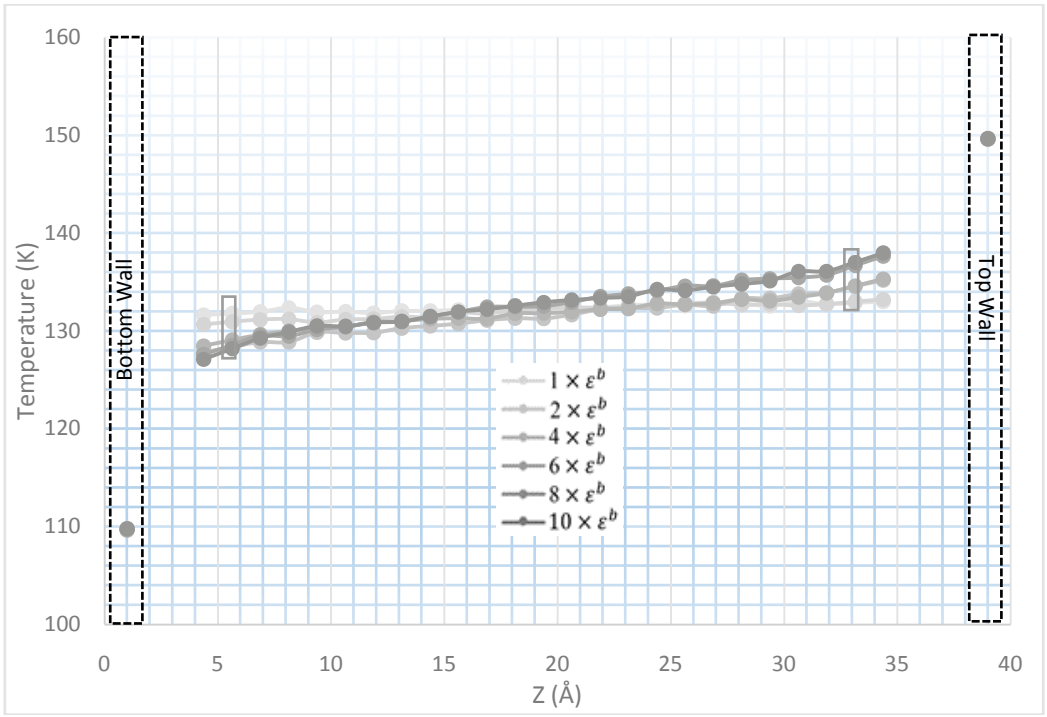

Figure 3: Temperature profiles of different values of wall-fluid interaction strength

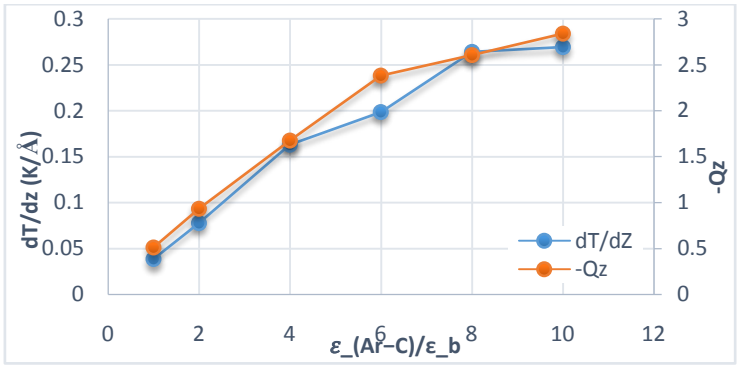

Figure 4: Temperature gradient of the bulk of Argon molecules and heat flux transferred between the walls for different values of wall-fluid interaction strength

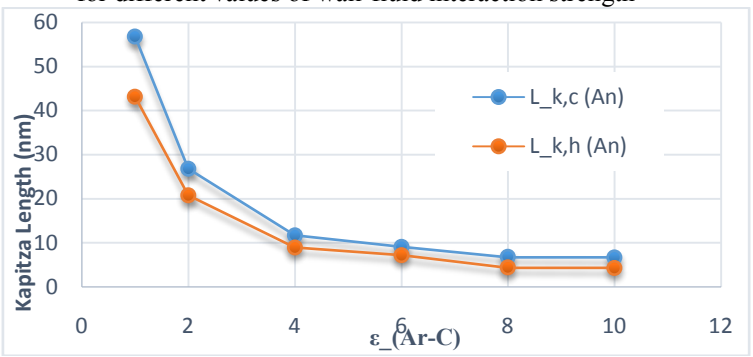

Figure 5: Kapitza length at liquid/solid interfaces for different values of wall-fluid interaction strength

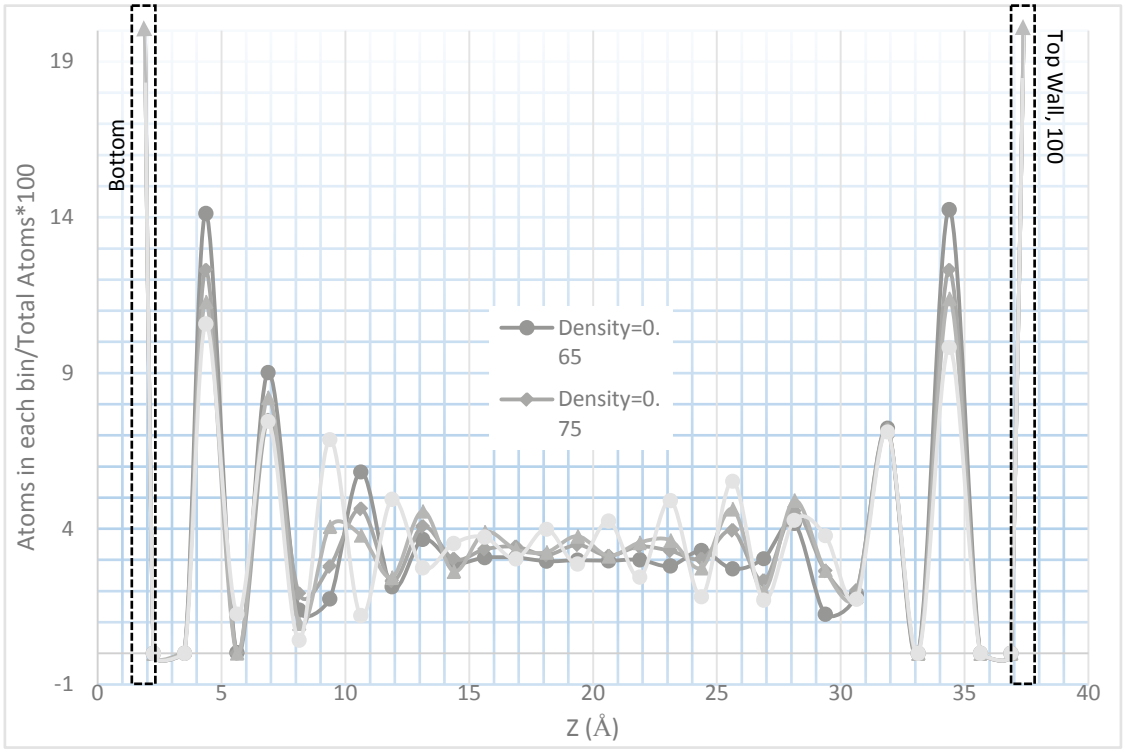

Figure 6: Proportion of the number of molecules in each bin to the total number of molecules for different particle densities

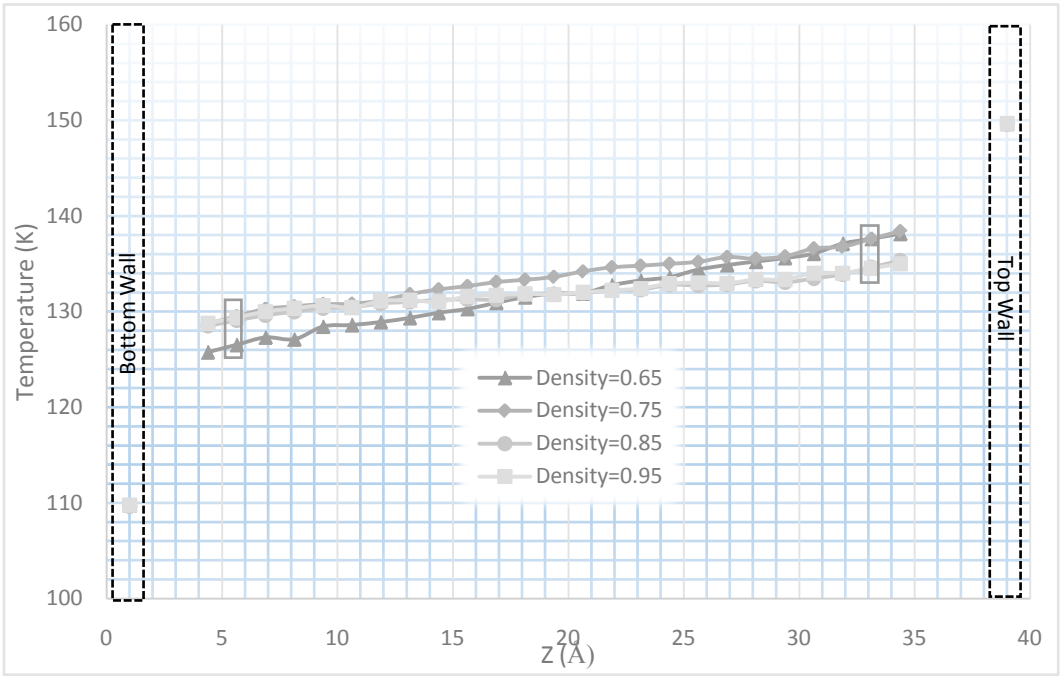

Figure 7: Temperature profiles of different values of particle densities

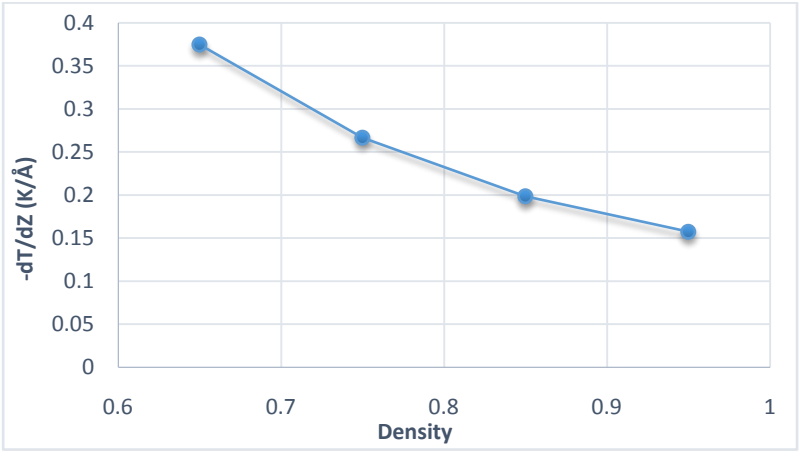

Figure 8: Temperature gradient of the bulk of Argon molecules for different fluid densities

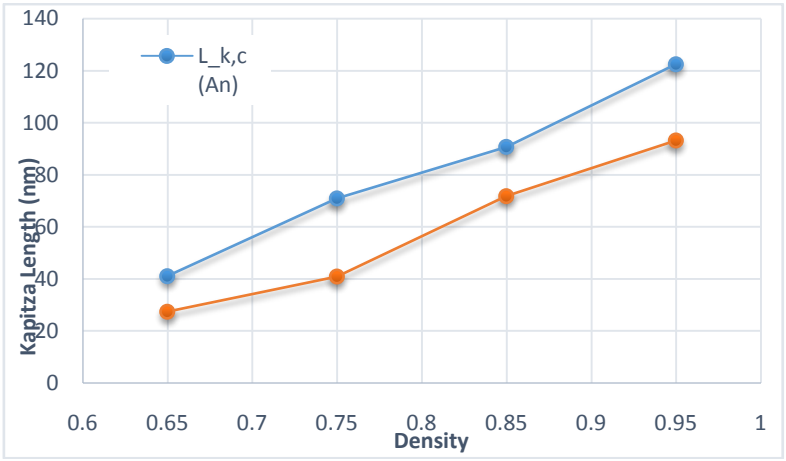

Figure 9: Kapitza length at liquid/solid interfaces for different fluid densities

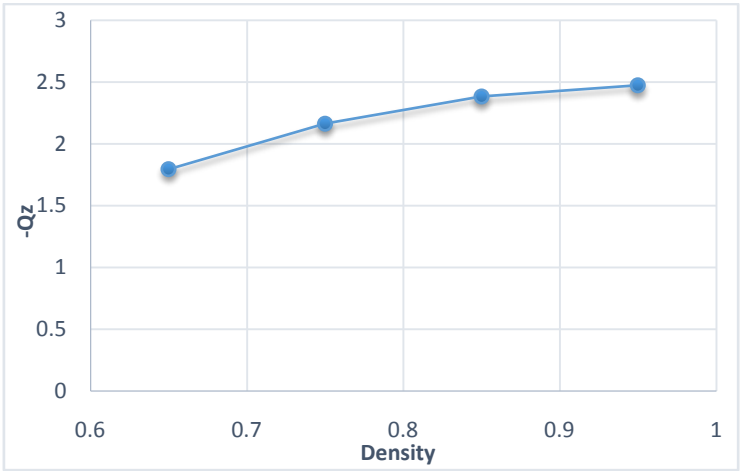

Figure 10: Heat flux generated between the walls for different fluid densities